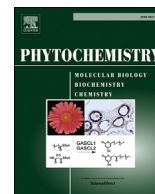




Contents lists available at ScienceDirect

Phytochemistry

journal homepage: www.elsevier.com/locate/phytochem

Isolation of isoflavones from *Iris kashmiriana* Baker as potential anti proliferative agents targeting NF-kappaB

Afroze Alam ^{a, **}, Varun Jaiswal ^a, Sohail Akhtar ^{b, c}, B.S. Jayashree ^d, K.L. Dhar ^{a, *}

^a Faculty of Pharmaceutical Sciences, Shoolini University, Solan, Himachal Pradesh 173229, India

^b LE STUDIUM® Loire Valley Institute for Advanced Studies, Centre-Val de Loire Region, France

^c Centre de Biophysique Moléculaire, CNRS UPR4301, Orléans, France

^d Manipal College of Pharmaceutical Sciences, Manipal University, Udupi, Karnataka 576104, India

ARTICLE INFO

Article history:

Received 4 September 2016

Received in revised form

30 December 2016

Accepted 4 January 2017

Available online xxx

Keywords:

Iris kashmiriana Baker

Iridaceae

Anticancer

Antioxidants

Cell cycle analysis

Docking study

G2/M phase

Isoflavonoid

NF-kappa B

ABSTRACT

Cancer is possibly one of the most devastating and complex disease and therefore involves chemotherapy as one of the frontline strategies in its therapy. However, expected toxicity and resistance with chemotherapeutic agents encourage us to use the plant derived natural chemotherapeutic sources at the clinical stage of cancer therapy. In view of this strategy, herein new glycosides and isoflavonoids were isolated from *Iris kashmiriana* Baker and subjected to structure elucidation followed by their biological evaluation. Isolated compounds and their derivatives were purified by the column chromatography and structural identification was made by a combination of various spectroscopic technique vis. UV, IR, ¹H NMR, ¹³C NMR, DEPT, 2-D NMR and mass spectrometry coupled with chemical analysis. Furthermore, an *in silico* library of isolated isoflavones and its analogues were designed. NF-kappaB (transcription factor that facilitates angiogenesis, inflammation, invasion and metastasis) was selected as a target to evaluate the anticancer and antioxidant activity of isoflavones and its analogues. Designed library of isoflavones and analogues were docked into the active site of NF-kappa B and the most active 15 analogues were selected for synthesis. Finally, all compounds were evaluated for their cytotoxicity against various cell lines and antioxidant activity with different methods that demonstrate their anti-cancer and antioxidant potential. The cell cycle specificity of the cytotoxicity was further analyzed by corresponding analysis, using flow cytometer. Most of the compounds exhibit moderate activity, whereas the 5,7,8-trihydroxy-3-(4-methoxyphenyl)-4H-chromen-4-one, 5,7,8-trihydroxy-3-(4-hydroxyphenyl)-4H-chromen-4-one, 5,7,8-triacetoxyoxy-3-(4-methoxyphenyl)-4H-chromen-4-one and 6,7-diacetoxyoxy-3-(4-methoxyphenyl)-4H-chromen-4-one showed distinct broad-spectrum anticancer activity with IC₅₀ values ranges between 3.8 and 5.6 µg/mL. Cell cycle analysis indicates that these compounds induced cell cycle arrest at G2/M phase.

© 2017 Elsevier Ltd. All rights reserved.

1. Introduction

Cancer is one of the most complex and challenging disease known to mankind and an inevitable public health concern. Chemotherapy is an essential component of cancer therapy. Yet, the present status of chemotherapy is far from being satisfactory. Its efficacy is limited and serious side effects are also associated with it, some of which are even life threatening (Akhter et al., 2013). The

number of new cases of cancer is expected to rise by about 70% over the next 2 decades (Bray et al., 2013). Safety concern to the cancer chemotherapy encourages the biomedical researchers and chemist to investigate the plant based natural chemotherapeutic agents. Several plant-derived anti-cancer agents, including taxol, vinblastine, vincristine, camptothecin derivatives; topotecan, etoposide etc. are in clinical use (Cassady et al., 2004). Other potential anti-cancer agents from this category include flavopiridol, roscovitine, combretastatin A-4, betulinic acid and silvestrol (Kingham, 1994). Cancer research in recent decade clearly illustrating that the plant based phytoactives particularly polyphenols such as flavonoids, isoflavonoids and their synthetic analogues are very effective against various cancers (Bray et al., 2013; Nadaroglu et al., 2007;

* Corresponding author.

** Corresponding author.

E-mail addresses: afrozepharma@gmail.com, afrozealam@shooliniuniversity.com (A. Alam), dharkl@yahoo.com (K.L. Dhar).

Williams et al., 1997; Arts and Hollman, 2005; Bhalla, 2003). Flavonoids and isoflavonoids are polyphenolic secondary metabolites which are widely present in our diet. These molecules contain broad-spectrum pharmacological activities including anti-cancer and anti-oxidant effects (Xiao et al., 2011). A positive correlation between isoflavonoids-rich diet and lower risk of various cancers have been reported in many studies (Bray et al., 2013; Nadaroglu et al., 2007; Williams et al., 1997; Arts and Hollman, 2005; Bhalla, 2003; Parr and Bolwell, 2000; Patel, 2008; Wallström et al., 2000; Xiao et al., 2011). Moreover, the antioxidant (Ali et al., 1983; Damme et al., 1997), antimicrobial (Bonfills et al., 2004; Kalla et al., 1977), anti-inflammatory and estrogenic activities (Kalla et al., 1977) of flavonoids and isoflavonoids have largely been acknowledged. Along with the conventional treatment (surgery, conventional chemotherapy and radiation therapy) of cancer, now a days cancer chemoprevention, by the use of natural, dietary or plant derived synthetic agents has become an appealing strategy (Tsao et al., 2004). It has been established that the one of the major mechanism of anti-cancer activity of flavonoids, isoflavonoids and their derivatives is inhibition of Nuclear factor kappaB (NF-kappaB) (Suthar et al., 2013). NF-kappaB is a transcription factor which plays a key role in carcinogenesis, immune and inflammatory regulation (Piccagli et al., 2010). Its carcinogenesis and immune regulatory effect comes from the combination of various effects such as NF-kappaB induced expression of genes that eventually promote cell proliferation, angiogenesis and stimulate invasion and metastasis (Perkins, 2007). Moreover, NF-kappaB activation is also considered as one of the factors behind chemotherapeutic and radiation resistance in cancers (Davis et al., 1999). Thus, flavonoids, isoflavonoids and their derivatives could be a potential cancer chemotherapeutic lead for the discovery of NF-kappaB inhibitors. NF-kappaB (nuclear factor kappa-light-chain-enhancer of activated B cells) is a protein complex that controls transcription of DNA (Brasier, 2006; Gilmore, 2006; Perkins, 2007; Tian and Brasier, 2003; Freudenthal and Romano, 2000; Levenson et al., 2004; Mattson and Camandola, 2001; Meffert et al., 2003; Merlo et al., 2002). Notably, NF-kappaB also blunts accumulation of reactive oxygen species (ROS), which themselves are pivotal elements for induction of PCD (Programmed Cell Death) by TNF alpha. Suppression of reactive oxygen species (ROS) mediates an additional protective activity as demonstrated recently is ascribed to NF-kappaB. Furthermore, Valachovicova et al. (2004) investigated the role of isoflavone aglycones (genistein, daidzein, glycitein) and their glucosides to reduce the mortality of MDA-MB-231 cell lines by targeting NF-kappaB (Piccagli et al., 2010; Cosconati et al., 2010).

Extraction and isolation of phytochemicals from the rhizome of *Iris kashmiriana* was carried out by usual process. The rationale for this selection was based on the fact that the highest number of isoflavones was found in the non-leguminous family (Iridaceae) of the genus *Iris*. Approximately more than two hundred compounds have been reported from the genus *Iris* which include flavonoids, isoflavonoids and their glycosides, benzoquinones, tri-terpenoids and stilbenes (Choudhary et al., 2001; Kachroo et al., 1990; Kalla et al., 1978; Nasim et al., 2003). *In silico* approach was used initially to design and syntheses of active molecules according to docking scores. Docking study of 30 possible analogues have been carried out against NF-kappaB active site. All the 30 possible molecules would have been generated by the usual process of hydrolysis; acetylation, per methylation, de methylation and esterification at different possible location of the both glycosides and its aglycones (Isoflavones). These possible molecules were virtually constructed and docked into the active site of NF-kappaB. Furthermore, according to the estimated free binding energy and interaction with the cavity residue of NF-kappaB, all the 30 molecules were ranked; the top 15 molecules were selected for analogue

synthesis. Finally, the anticancer and anti-oxidant activity of previously undescribed glycosides, aglycones (isoflavones) and its analogues were evaluated against different cell lines, namely MCF-7, MDA-MB-231, PC-3, A-549, *HeLa* and Vero cell lines. Furthermore, it is indeed difficult to imagine the possible biochemical mechanism of the anticancer action of natural products. A common activity noted for most of such products is that they act as potent antioxidants and free radical scavengers (Colic and Pavelic, 2000). Plants contain certain chemicals such as carotenoids, flavonoids, isoflavonoids, bioflavonoids, phenols, phytosterols etc. that possess antioxidative properties. Since reactive oxygen radicals play an important role in carcinogenesis and other human disease states, antioxidants present in plants have received considerable attention as cancer chemopreventive agents (Lee et al., 1998). Compounds showing promising cytotoxic activities in selected cell line (MCF-7) were further subjected to cell cycle analysis using flow cytometer. According to flow cytometric analysis most of the molecules (four out of six) have shown to induce cell cycle arrest at G2/M phase. An attempt was made to establish structural activity relationships (SARs) of compounds against proposed activity to develop new lead molecules and SAR was in accordance with computational as well as wet lab results. Around 85% of the *in silico* results matched with the wet lab experiments which clearly indicates the importance of computer aided drug design in the development of novel molecules. However, *in vivo* study would be the future prospect for further study. The present study clearly indicates the significance of (1b) and (1g) as potent anticancer or/and antioxidant agent and must be further considered for preclinical and clinical studies.

2. Result and discussion

Extract from rhizome of *Iris kashmiriana* Baker was prepared with 95% methanol. Further, bioactivity-guided fractionation in *n*-butanol fraction resulted in isolation of two glycosides. Thirteen analogues were synthesized from isolated glycosides. Details of chemical and spectroscopic characterization of glycosides and its analogues (fifteen compounds) are discussed here.

2.1. Glycoside I

Glycoside-1 was obtained as a white crystalline solid through repeated column chromatography followed by crystallization in methanol. The melting point of the compound was 285–290 °C. The elemental analysis was found (%) C; 57.14, H; 4.80, O; 38.06 and required; C; 57.02, H; 5.07, O; 37.96. Mass spectrometry analysis by TOF, MS, ES⁺ (*m/z*) showed 463.5 molecular wt. Further, information about the compound was obtained from ¹H NMR (400 MHz, δ, DMSO, TMS = 0); Methoxy group was present at 3.87 as a sharp singlet at C-4' position in ring-B. The ring B has two doublet at 6.85 (2H, d, 3',5'-H, *J* = 8.56 Hz), and 7.37 (2H, d, 2',6'-H, *J* = 8.56 Hz), which indicate that there is no other groups attached to the ring B. The anomeric hydrogen atom of the sugar was located at 5.02 (*J* = 7.52 Hz), which indicates the presence of sugar molecule linked at the C-7 position, further presence of sugar could be easily identified by the presence of protons between 3.33 and 3.64. There is only one signal at 6.79 due to C-6 of ring A. This also indicates that the carbon number C-5, C-7 and C-8 are occupied with different functional groups. There is sharp singlet at 8.17 for a C-2 proton. A downfield singlet at 12.92 exchangeable with D₂O was attributed to phenolic proton. U.V. Shift with AlCl₃ confirmed the presence of hydroxyl groups at C-5, while the absence of sodium acetate shift indicated the C-7 and C-4' hydroxyl were substituted. The structure was further assigned by ¹³C NMR, discussed in experimental section. IR revealed the prominent peak at 3365 cm⁻¹ (Ar-OH), 1659 cm⁻¹ (>C=O). From UV, IR, ¹H NMR, ¹³C NMR and mass

spectral data the structure was assigned as 7-O- β -D-Glu-5, 8-dihydroxy-4'-methoxyisoflavone. Acetylation of (**1**) gave a hexaacetate (**1a**). In the ^1H NMR (DMSO) of (**1a**), all the signals of the aromatic protons remain unchanged except the four acetate groups present on glucose, two acetate group at C-5 and C-8, and downfield displacement of the signal for the C-6 proton from 6.79 to 7.07 indicating the two hydroxyl groups were present at C-5 and C-8, whereas the C-7 was linked with glycosidic bond in ring A. Acid hydrolysis followed by column chromatography of (**1**), yielded glucose and an aglycone (**1b**). The structure 5,7,8-trihydroxy-4'-methoxyisoflavone (**1b**), was established by ^1H NMR, ^{13}C NMR, 2-D NMR and mass spectrometry. In the ^1H NMR (DMSO) of (**1b**) there is a sharp up field displacement of the signal at C-6 proton from 7.07 to 6.44 revealed the establishment of structure (**1b**) as novel aglycone. The acetylation of (**1b**) gave 5, 7, 8 - triacetate isoflavone (**1c**). The identification and establishment of the structure was proved by IR, ^1H NMR, ^{13}C NMR, 2-D NMR and mass spectrometry. The IR revealed a strong peak of phenol acetate at 1760 cm^{-1} . In the ^1H NMR (CDCl_3) of (**1c**); all the signals remain unchanged except the downfield displacement of the signal for the C-6 proton from 6.46 to 7.19 indicating the three hydroxyl groups were present at C-5, C-7 and C-8, and on acetylation gave triacetate. Further three acetate groups confirmed by ^1H NMR (CDCl_3) at 2.31, 2.38, 2.46 correspond to nine protons singlet. The position of glycosidic linkage was further confirmed by the per methylation of (**1**) to yield (**1d**) which on subsequent acid hydrolysis yielded (**1e**) and identified as 7-hydroxy-5,8,4'- tri-methoxy isoflavone. The aglycone was isolated, purified and recrystallized with methanol as a compound (**1e**) having m.p. 243–245 °C and further analyzed for $\text{C}_{18}\text{H}_{16}\text{O}_6$. It was identified by ^1H NMR, (DMSO δ with TMS = O) and mass spectrometry as 7-hydroxy-5, 8, 4'-trimethoxy isoflavone. ^1H NMR (DMSO δ with TMS = O) showed three methoxyls at 3.983, 3.886, 3.857 assigned to C-5, C-8 and C-4' position respectively. A singlet at 6.485 could be assigned to C-6 proton beside two doublets ($J = 8.1\text{ Hz}$ each) at 6.845 and 7.359 for two protons each of 3', 5' and 2', 6' proton respectively. C-2 proton as singlet appeared at 8.157. The acetate of (**1e**) aglycone was obtained by adding acetic anhydride and a few drops of H_2SO_4 and assigned as (**1f**) white crystalline m.p. 195–198 °C showed a down field shift of C-6 proton to 7.193 indicating unambiguously that free hydroxyl group is at C-7 and therefore sugar moiety was fixed to the new isoflavone. A bathochromic shift in the peaks from 341.6 nm to 377.6 nm and 238.4 nm to 264.8 nm, respectively in UV in presence of aluminium chloride indicating two free hydroxyl groups located at C-5 and C-8, leaves only the C-7- position for glycosylation in ring A. Acetylation of (**1e**) gave (**1f**), identified as 7-acetyl-5,8,4'- tri-methoxy isoflavone, which is confirmed by ^1H NMR (CDCl_3) with 2.463 singlet for three protons indicating the presence of acetate groups at the C-7 position in ring A. The (**1b**) was subjected to de methylation by HBr to yield (**1g**), that contain a hydroxyl group at C-4' position. The structure was identified and confirmed by ^1H NMR (CDCl_3) at 12.930 singlet exchangeable with D_2O instead of the methoxy group at C-4' position in ring B.

2.2. Glycoside-II

The second glycoside and its analogues (isoflavone) were assigned as series of glycosides II (**2**), based on their chemical and spectral analysis. There is no any UV spectral shift with aluminium chloride and sodium acetate, ascertained the presence of the free hydroxyl group at C-6 instead of C-5. It was further confirmed by IR, ^1H NMR, ^{13}C NMR and mass spectrometry analysis. IR analysis displayed a band at 1648 cm^{-1} ($>\text{C}=\text{O}$) and 3340 cm^{-1} (Ar–OH). ^1H NMR (DMSO) showed a sharp singlet for one methoxy group at 3.87 due to proton of C-4' in ring B. The ring B has two doublet at 7.36

and 6.84, with J value of 8.56 Hz integrating for two protons at C-2'; C-6'; C-3' and C-5' respectively. A sharp two singlet for two protons at 8.24 and 8.02 was assigned to the C-2 and C-5 respectively. A singlet at 6.81 for one proton assigned to C-8. A doublet at 5.03 ($J = 7.58\text{ Hz}$) integrating for a single proton was assigned to C-1'' proton of a sugar moiety also indicating a β – linkage. A downfield singlet at 12.92 exchangeable with D_2O was attributed to phenolic proton. Acetylation of (**2**) followed by subsequent acid hydrolysis gave (**2a**). Acetylation has only taken place at C-6 while no acetylation took place at C-7 as proving that sugar is attached to C-7. In the ^1H NMR (DMSO) of (**2a**), all the signals remain unchanged except for a downfield displacement of the singlet for the C-5 proton from 8.02 to 9.50 indicating the hydrogen bonding exists between the free hydroxyl group on C-7 and acetyl group at C-6. The extraordinary down field of C-5 is due to the fact that the C-5 proton comes in two carbonyl ($>\text{C}=\text{O}$) double bonds of C-4 ($>\text{C}=\text{O}$) and C-6 ($>\text{C}=\text{O}$) besides the strong hydrogen bonding between C-6 and C-7 in ring A. The hydrogen atom present at C-8 has shown an up field at 6.48 (1H,s, 8-H) indicate the presence of hydroxyl group at C-7 and the linkage of sugar to C-7. A sharp singlet for one proton at 8.28 comes from C-2 proton. IR spectra revealed a strong peak at 1758 cm^{-1} ($>\text{C}=\text{O}$) and 3360 cm^{-1} (Ar–OH) indicating the presence of the acetyl group specific to the phenolic acetate. Further structure was assigned by ^{13}C NMR. (Discussed in experimental section). Finally, the (**2a**) structure was assigned as 7- hydroxy-6-acetyl-4'-methoxy isoflavone. Acid hydrolysis followed by subsequent acetylation of (**2a**) gave (**2b**). In the ^1H NMR (DMSO) analysis, all the signals remained unchanged except for an up field displacement of the singlet for the C-8 proton from 6.81 to 6.48, indicates that glycosidic linkage was present at C-7 in ring A. A complete acid hydrolysis of compound (**2**) yielded an aglycone (**2c**). In (**2c**), as expected there is only difference appeared at C-5 and C-8 where up field ^1H NMR (DMSO) signals were present. This indicates the presence of hydroxyl groups at C-6 and C-7 position in ring A. Furthermore, it has been concluded that the glycosidic linkage was present at C-7 position of ring A. The position of glycosidic linkage was further confirmed by the per methylation of (**2**) to (**2d**) that on subsequent acid hydrolysis gave (**2e**) followed by acetylation yielded (**2f**) and identified as 6,4'-di-methoxy-7-acetyl isoflavone by chemical and spectral data analysis. The ^1H NMR (DMSO) of (**2e**) showed an up field displacement of the singlet for the C-8 proton at 6.48 indicating the presence of the glycosidic linkage at C-7 in ring A. No bathochromic shift has been observed in UV with aluminium chloride indicating no free hydroxyl group present at C-5, leaves only the 7- position for glycosylation. In the ^1H NMR (DMSO) of (**2f**) showed two sharp singlet (integrating each of three acetyl protons) at 3.83 and 3.92 present at C-4' and C-6 respectively, further one acetate group was confirmed by ^1H NMR (DMSO) integrating for three protons singlet at 2.51 at the C-7 position in ring A. There is one singlet at 6.48 for the C-8 proton. A singlet at 8.16 for one proton assigned to C-5 indicating the presence of the methoxyl group at C-6. The IR revealed a strong peak at 1755 cm^{-1} which is characteristics of phenol acetate. The ester bond was further confirmed by a strong peak at 1180 cm^{-1} . From above observation the structure was assigned as 6, 4'-dimethoxy-7-acetyl isoflavone (**2f**).

2.3. Biological activity

Isolated glycosides and its analogues were subjected to antioxidant activity through DPPH and ABTS and anticancer activities against various cell lines.

2.3.1. Antioxidant activity

The *in vitro* antioxidant study revealed that most of the

Table 1
IC₅₀ of isolated compounds and its analogues towards antioxidant by DPPH and ABTS screening method.

Compound	IC ₅₀ µg/mL ^a	
	DPPH (µg/mL)	ABTS (µg/mL)
1	32.4	105.7
1a	34.8	145.6
1b	08.3	24.4
1c	10.9	26.1
1d	24.6	47.5
1e	19.7	38.2
1f	20.5	41.9
1g	09.8	26.7
2	54.1	150.4
2a	11.3	28.5
2b	16.8	41.3
2c	10.4	27.9
2d	56.0	167.3
2e	11.5	27.3
2f	13.2	32.6
Ascorbic acid^b	5.63	15.97

^a Average of three determinations.

^b Standard drug.

compounds are moderately active (Table 1), whereas two compounds; (**1b**) (8.3 µg/mL DPPH and 24.4 µg/mL ABTS) and (**1g**) (09.8 µg/mL DPPH and 26.7 µg/mL ABTS) shown remarkable high antioxidant activity. Promising activity of these two compounds is believed to be due to the presence of hydroxyl groups at C-7, C-5, and C-8 positions in ring A, and one methoxyl group at C-4'-position in ring B. As shown in Fig. 1A, the structures of (**1b**) and (**1g**) were different from each other only by the presence of 4'-OMe and 4'-OH respectively, nevertheless their IC₅₀ were found to be nearly the same (Table 1). However, in molecule (**1c**) the presence of acetyl groups at C-7, C-5, and C-8 with no other key substituents, showed considerably lower activity, suggesting that electron withdrawing substituents attached to the oxygen function reduces the antioxidant activity as expected. (**2c**) an aglycone also showed a comparable level of antioxidant activity (10.4 µg/mL DPPH and 27.9 µg/mL ABTS) indicating that the presence of two hydroxyl groups at C-7, C-6-position in ring A, were important for its activity. The absence of free OH substituents at ring A & B rendered the isoflavone and its analogues completely inactive for antioxidant activity. (**1e**) and (**1f**) have exhibited moderate antioxidant activities (19.7 µg/mL DPPH and 38.2 µg/mL ABTS, 20.5 µg/mL DPPH and 41.9 µg/mL ABTS) where the hydroxyl groups are replaced by the methoxy group at C-5, C-8 and C-7 positions. However, in (**1f**) the only difference occurs at the C-7 position where the hydroxyl group was replaced by acetate group. The results, however, showed much weaker activity for (**1**),

(**2**), (**2d**) and (**1a**), suggesting that these glycosides and acetylated glycoside were not as important. From the results, it was concluded that the -OH substitutions at C-5, C-7 and C-8 of ring A and either -OMe or -OH substitution at C-4' of ring B in the isolated compounds and its analogues promote oxygen radical scavenging capacity. The replacement of -OH substituents with -OCOCH₃ or -OMe significantly reduces the antioxidant activity. Thus, among the free OH substitution, the positions of the C5-OH, C7-OH and C8-OH of ring A and C4'-OH of ring B appeared to be important.

2.3.2. In vitro cytotoxic studies (MTT assay)

The cytotoxic effect of isolated compounds and its analogues were evaluated in various cancer cell lines vis. MCF-7, MDA-MB-231, HeLa, A-549 (Lung Cancer), PC-3 (Prostate cancer), and Vero (Normal kidney epithelial cell line). The obtained IC₅₀ values of for the tested compounds are presented in Table 2. Comparative anti-cancer activity based on their SAR is discussed here. The compounds have shown promising cytotoxicity in different cell lines were (**1b**), (**1g**), (**1c**), (**2b**), (**1d**) and (**2c**). Compound (**1b**) and (**1g**) were appeared to be more potent among all, as these compounds, had common substituent patterns; the presence of hydroxyl groups at C-8, C-7 and C-5 position of ring A, and methoxy or the hydroxyl group at C-4' position in ring B. In terms of substituents, it also suggests that -OH groups are important for the inhibitory effect. In fact, the simultaneous presence of both hydroxyl and methoxy groups were particularly important and responsible for their potent cytotoxic activity. The significant cytotoxic activity of the compounds ((**1b**) and (**1g**)) were also attributed due to the structural resemblance with genistein and daidzein, (Valachovicova et al., 2004). Furthermore, the analysis of the position of substituents in molecule (**1c**) of ring A, interestingly, revealed that the replacement of hydroxyl groups with acetyl groups at C-5, C-7, C-8 showed considerably lower activity, suggesting that electron withdrawing groups are not as important, rather reduces the activity. The absence of oxygen functionality in any of the ring caused the complete loss of the activity. It can be observed in the molecule (**2c**) an aglycone also exhibited a comparable level of cytotoxic activity with (**1b**) and (**1g**), presumably, due to the presence of two hydroxyl groups at C-7, C-6- position in ring A. Based on the cytotoxic results, mentioned in Table 2, it was concluded that in the molecule (**1d**), the sugar moiety linked at C-7 and the replacement of hydroxyl groups with methoxy groups at C-5 and C-8 group of ring A led to significant reduction of anti-proliferative activity. The results showed that compounds with the linkage of the sugar moiety at C-7 position of the ring A did not show any notable cytotoxicity against all the cell lines, indicating the hydroxyl groups should remain unprotected (see Table 2).

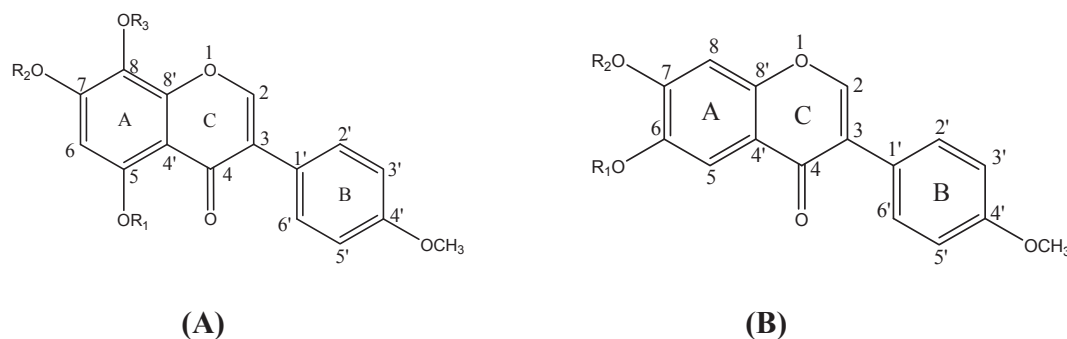


Fig. 1. (A) & (B) Structure of glycoside-I & II and their aglycones (Isoflavones). **Fig 1(A); Glycoside-I. 1** R₁ = H, R₂ = Glu, R₃ = H; **1a**) R₁ = -OCOCH₃, R₂ = Glu, R₃ = OCOCH₃; **1b**) R₁, R₂, R₃ = H; **1c**) R₁, R₂, R₃ = OCOCH₃; **1d**) R₁ = OCH₃; R₂ = Glu R₃ = OCH₃. **1e**) R₁ = OCH₃; R₂ = -OH, R₃ = OCH₃; **1f**) R₁ = OCH₃; R₂ = OCOCH₃ R₃ = OCH₃. **1g**) R₁, R₂, R₃ = H; **Fig 1(B); Glycoside-II. 2**) R₁ = H, R₂ = Glu, **2a**) R₁ = -COCH₃, R₂ = H **2b**) R₁, R₂ = -COCH₃ **2c**) R₁, R₂ = H **2d**) R₁ = CH₃; R₂ = Glu **2e**) R₁ = CH₃; R₂ = H, **2f**) R₁ = CH₃; R₂ = -OCOCH₃. Glu = Glucose.

Further moderate cytotoxic activity of compounds ((**1e**), (**1d**), (**1f**), (**2f**) and (**2d**)) revealed that cytotoxic activity was depend not only on the number of phenolic hydroxyl groups, but also on various factors such as their structures, hydrophobic properties, and hydrophilic properties.

The present study reveals that substitution patterns at C-4' in ring B and C-5 C-7 and C-8 in ring A with the oxygen functionality of novel isoflavones were found to be the most promising and more selective towards NF-kappaB (with IC₅₀ values 3.8–4.9 µg/mL). Their results also indicate the cytotoxic activity might be due to the inhibition of NF-kappaB signaling. Suthar et al. (2013) found that inhibition of NF-kappaB potentiate the anticancer effect of chemotherapeutic agents. The docking study results of six top ranked tested compounds (**1b**), (**1g**), (**1c**) (**2b**), (**1d**) and (**2c**) have shown a direct correlation ship of NF-kappaB inhibition with

anticancer activity against different cancer cell lines (MCF-7, MDA-MB-231, HeLa, and A-549, Vero (Normal kidney epithelial cell line). It has been concluded that (**1b**) and (**1g**) have shown highest free energy of binding (–32.50 and –31.96 kJ/mol respectively), was in correlation with activity in wet lab experiments (Figs. 3 and 4). The top ranked compounds were subjected to cell cycle analysis using flow cytometer and have shown to induce cell cycle arrest mainly at G2/M Phase (Kong et al., 2010). Based on these results, it was concluded that the –OH substitutions at C-5, C-7 and C-8 of ring A and presence of –OMe or –OH at C-4' of ring B in the compounds have similar receptor interaction with N F-kappaB as the natural compounds genistein and daidzein (Borgatti et al., 2011). These isoflavone have already been proven to elicit pronounced cell inhibitory activity against different cancer cell lines through inhibition of transcription signals of NF-kappaB (Piccagli et al., 2009). Novel isoflavones were isolated and subjected to analogue synthesis. Further anticancer activity of isoflavone and its analogue revealed promising anticancer activity of some of the compounds. Compounds with promising activity were selected for further cell cycle analysis to explore the mechanism of anti-cancer activity.

Table 2

IC₅₀ of isolated compounds and its analogues towards various cell lines by MTT assay method, after 48 h.

Compound	IC ₅₀ µg/mL ^a					
	MCF-7	MDA-MB -231	PC-3	HeLa	A-549	Vero
1	50.1	47.5	48.1	>200	>200	>1000
1a	22.0	24.6	37.5	150.2	176.2	>1000
1b	03.8	04.7	05.7	04.9	04.8	>1000
1c	05.2	07.9	08.2	16.5	14.8	>1000
1d	05.4	08.4	10.2	08.1	08.4	>1000
1e	18.9	19.6	19.2	21.6	32.8	>1000
1f	10.5	15.2	22.7	39.3	38.9	>1000
1g	04.1	04.9	05.6	05.3	04.6	>1000
2	42.0	31.0	63.1	82.6	73.8	>1000
2a	07.2	10.6	07.4	23.5	10.7	>1000
2b	05.3	08.0	07.1	06.5	05.8	>1000
2c	07.8	09.5	10.2	07.7	06.7	>1000
2d	14.3	12.8	14.7	36.6	45.6	>1000
2e	06.2	08.6	11.2	17.9	26.5	>1000
2f	17.3	21.5	41.5	37.8	35.7	>1000
DOXO	2,356	3,742	4,513	4,894	3,589	550.

Doxo = Doxorubicin; Standard Anticancer Drug.

^a Average of three determinations.

2.4. Cell cycle analysis

The compounds ((**1b**), (**1g**), (**1c**), (**2b**), (**2c**) and (**2d**)) were subjected to cell cycle analysis against MCF-7 cells. Isoflavone and its analogues had maximum anti-cancer activity on MCF-7 cell line among all cell lines used in the study. Hence, MCF-7 used for cell cycle analysis. In control the percentage inhibition of cells in G0/G1 phase is 50.2%, S phase is 14.4% and G2/M phase is 25.5%. In case of Standard Drug (Doxorubicin) MCF-7 Cell the percentage inhibition of cells in G2/M phase has increased to 34% and decreased to 38.6% in the G0/G1 phase compared to the control cell lines. Hence doxorubicin has been shown to induce cell cycle arrest at the G2/M phase as shown in Fig. 2 B. For compound- (**1b**) the percentage arrest of the cells in G2/M phase has increased to 33.5% and decreased to 41% at the G0/G1 phase. Hence (**1b**) has been shown to induce cell cycle arrest at the G2/M phase. There is a marked increase in percentage arrests of the cell to 28% at the S phase, indicating that (**1b**) induces

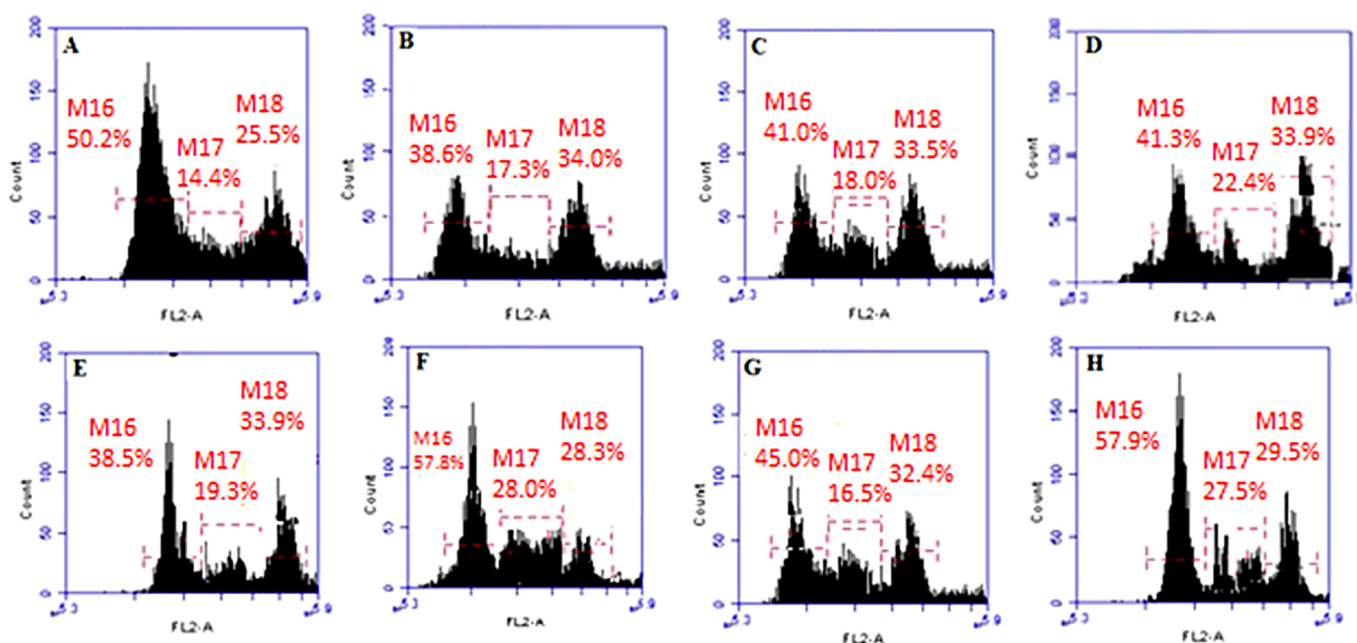


Fig. 2. Effects of test samples (Equal concentration; 100 µg/mL) treatment on cell cycle against negative (untreated cells) and positive control (Doxorubicin). (A) Negative control, (B) Positive control, (C) 1b, (D) 1g, (E) 1c, (F) 2b, (G) 1d, (H) 2c. The study was performed by flow cytometer keeping rest of the parameters constant for each sample.

the cell cycle arrest in the S phase. In compound (**1g**) the percentage arrest of the cells in G2/M phase has increased to 33.90% and decreased in the G0/G1 phase to 41.3% compared to the control cell lines. Hence (**1g**) has shown cell cycle arrest at G2/M phase. In the compound (**1c**) the percentage arrest of the cells at G2/M phase has increased to 33.9% and decreased to 38.5% at the G0/G1 phase in comparison to control cell lines. Hence (**1c**) has been shown to induce cell cycle arrest at the G2/M phase. There is also increased in the percentage arrest of the cell to 19.3% at the S phase compared to the normal cell, which indicates that (**1c**) also has been shown to induce cell cycle arrest at the S phase. In (**2b**) the percentage arrest of the cells in G2/M phase has increased to 28.3% and G0/G1 phase to 57.8%. Hence (**2**) has been shown to induce cell cycle arrest at the G0/G1 phase. There is some increase (28.3%) in the percentage arrest of the cell at the G2/M phase, which indicates that (**2b**) has shown cell arrest at the G2/M phase.

In compound (**1d**) the percentage arrest of the cells at G2/M phase has increased to 32.4% and decreased to 45% at the G0/G1 phase. Hence (**1d**) has been shown to induce cell cycle arrest at the G2/M phase. In compound (**2c**) the percentage arrest of the cells in G2/M phase has increased to 29.5% and 57.9% at the G0/G1 phase in comparison to the control cell lines. Hence (**2c**) has shown cell cycle arrest at the G2/M phase and some arrest has also been shown in G0/G1 phase. It is important to mention that a different site of cell cycle arrest has been suggested for the different analogues of isoflavone, based on their cell cycle arrest data (Bhalla, 2003; Walle,

2007; Yarishkin et al., 2008).

2.5. Drug receptor interaction study

Ligands were ranked according to docking score/estimated free energy of binding. The free energy of binding of ligands was in the range between -25.94 and -32.50 KJ/mole. Top ranked compound (**1b**) and (**1g**) with -32.50 and -31.96 KJ/mole free energy of binding, respectively, were in correlation with wet lab experiments. The protein ligand analysis also has shown its strong interactions with target protein and had five hydrogen bond interaction in (**1b**) and six hydrogen bond interaction in (**1g**). The residues involved in hydrogen bond interaction were Gln 274, Gln 306, Arg 305, Lys 275 and Asp 276 in (**1b**) (Fig. 3) and Ser 303, Ser 347, Thr 352, Thr 355, Asp 347 and Glu 488 in (**1g**) (Fig. 4) with the active site of NF-kappaB. Virtual screening of various isolated isoflavone and its analogue library resulted in the identification of 30 compounds. Out of 30 compounds, 15 compounds with the higher estimated free energy of binding were selected for analogue synthesis. Among synthesized compounds top ranked compounds (**1b**) and (**1g**) according to estimated free energy of binding (-32.50 and -31.96 kJ/mol respectively), also had promising anti-oxidant and anti-cancer activity in wet lab experiments. Our group followed same docking procedure of NF kappa B in earlier study and docking score were in correlation. Similarly in current study docking score were in correlation with experimental results which validate the virtual

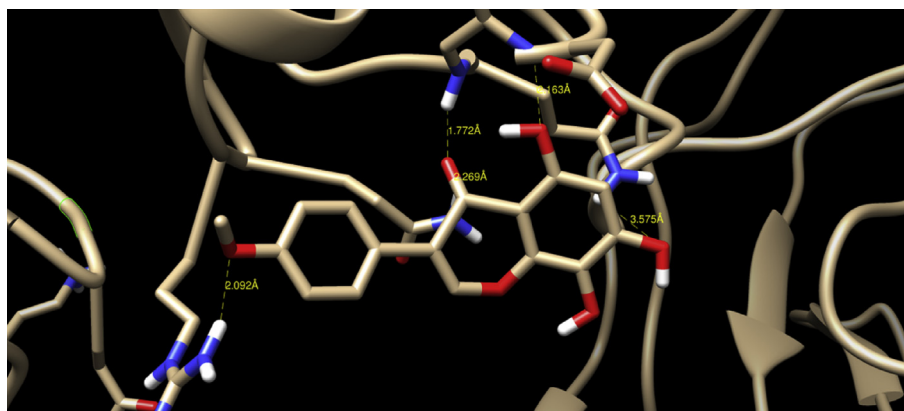


Fig. 3. Stereoview of the complex formed by NF-kappaB and the docked compound (**1b**). The amino acids Gln 274, Gln 306, Arg 305, Lys 275 and Asp 276 were involved in interaction with compounds.

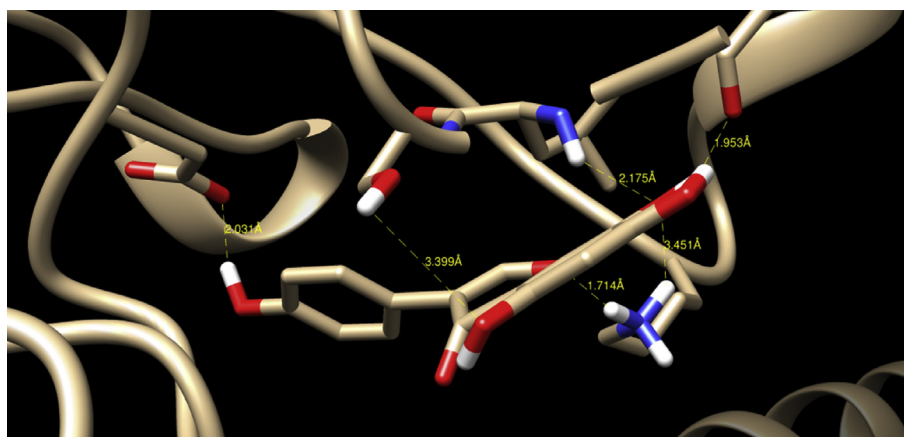


Fig. 4. Stereoview of the complex formed by NF-kappaB and the docked compound (**1g**). The amino acids Ser 303, Ser 347, Thr 352, Thr 355, Asp 347 and Glu 488 were involved in interaction with compounds.

Table 3

Estimated free energy of binding of isolated compounds in the target NF-kappaB as homo dimer (p50-p50).

Compounds	Estimated free energy of binding (kJ/mol)
1b	–32.50
1g	–31.96
1c	–31.84
2b	–30.29
1d	–29.95
8	–29.95
9	–29.32
2c	–28.66
2f	–28.61
5	–28.49
11	–28.13
1f	–27.86
10	–27.36
15	–27.27
2e	–27.07
14	–26.86
1e	–26.06
4	–25.98
3	–25.94

3D structures of NF-kappaB, p50-p50 homo dimer (from 1NFK), was used for virtual screening.

docking studies (Suthar et al., 2013). The excellent interactions of NF-kappaB with all five top ranked compounds (**1b**), (**1g**), (**1c**), (**2b**) and (**1d**) indicated a high degree of coherent relationship between *in silico* approach and *in vitro* studies. Large number of hydrogen bond interaction that exists between different amino acid of the NF-kappaB and novel isoflavones were mainly due the hydroxyl/methoxy group present in ring A and B. As the test compounds inhibits transcriptional factors NF-kappa B, that supports the results of cell cycle analysis in which induction of cell cycle arrest mainly take place at G2/M Phase (Bhalla, 2003). The recent study has indicated that NF-kappa B also protects cells against TNF-R-induced cytotoxicity by controlling the accumulation of ROS induced downstream of these receptors (Kamata et al., 2005). High anti-cancer and anti-oxidant of the compounds (isoflavone and its analogues) demands further *in vivo* and clinical studies and these compounds might find an important place in the new array of molecules targeting NF-kappaB dependent biological functions as anti-oxidant and anticancer agents (Table 3).

3. Conclusion

A new series of isoflavones were isolated from *Iris kashmiriana* Baker and further its analogues were synthesized and characterized (Chemical & Spectroscopic methods). Syntheses of isoflavone analogues were carried out according to *in silico* docking score. *In vitro* screening of isolated isoflavones and its analogues were carried out for anti-cancer activity using NF-kappa B as a target and antioxidant activity. Isolated isoflavones and its analogues showed excellent interactions with NF-kappaB and established a high correlation between *in silico* score and *in vitro* anti-cancer study. Most of the compounds illustrated a fair anti-cancer activity in different cancer cell lines. Among them, the compounds (**1b**) and (**1g**) have shown marked, broad-spectrum anticancer activity by inducing the cell cycle arrest at G2/M phase. Promising activity of these compounds ((**1b**) and (**1g**)) demands further *in vivo* and clinical studies.

4. Experimental

The rhizomes of *Iris kashmiriana* Baker were collected from the wild accessions growing in Parvati Valley in district Kullu, Himachal Pradesh, India, at an elevation of 3500–4000 m above sea level

during the month of Aug.–Sept. 2012 and duly authenticated by Dr. R Raina, Senior Scientist/Professor (Medicinal Plants), Department of Forest Products, Dr Y. S. Parmar University of Horticulture and Forestry, Nauni 173230, Solan (HP) India, linked to UHF– Herbarium with Field Book No: 12566.

4.1. Extraction and isolation

The rhizomes of *Iris kashmiriana* Baker were dried chopped and powdered (500 g). The extraction of powdered drug was done with petroleum ether (60–80 °C) using soxhlet apparatus (24 h run). The petroleum ether extract (gums and resins 2.13 g) was obtained and the marc was subjected to extraction with methanol using soxhlet apparatus (24 h run). The methanolic extract (5 g) was subjected to successive fractionation with toluene, chloroform and ethyl acetate and n- butanol. The phytochemical screening of each extract and fraction were done. On the basis of phytochemical screening results, the glycosides were present in n- butanol fraction. Column chromatography was performed with n-butanol fraction in chloroform: methanol (9:1) as solvent system. Fractions (1–100) were collected and TLC (Thin Layer Chromatography) was observed, three different single spots were found in the range of 40–50, 55–60 and 85–100 test tubes respectively. The identical TLC pattern ones were pooled. All the melting points found were uncorrected ¹H NMR, ¹³C NMR was recorded on BRUKER AVANCE II 400 NMR Spectrometer SAIF Punjab University, Chandigarh, using CDCl₃/DMSO as solvent with TMS as internal standard. Phytochemical tests were performed and following compounds were identified in n-butanol fraction.

4.2. Glycoside (1) 7-((2S,3S,4R,5S)-tetrahydro-3,4,5-trihydroxy-6-(hydroxymethyl)-2H-pyran-2-yloxy)-5,8-dihydroxy-3-(4-methoxyphenyl)-4H-chromen-4-one

White solid crystalline mass was obtained in n-butanol fraction and was further crystallized from methanol, which was appeared to be a glycoside **1g**, assigned as (**1**), melting point 285–290°C and analyzed for C₂₂H₂₂O₁₁. **TOF MS ES⁺** (m/z): 463.5. Elemental Analysis Found (%): C; 57.14,H; 4.80,O; 38.06 and Required: C; 57.02,H; 5.07,O; 37.96. Further the structure was confirmed by UV, IR, ¹H NMR, and ¹³C NMR. The λ_{max} was determined by UV. in different solvents and appeared as changed in λ_{max} (341.6 nm, 238.4 nm in methanol, 377.6 nm, 264.8 nm in methanol + AlCl₃, and 377.6 nm, 264.8 nm in methanol + AlCl₃ HCl). **IR (cm⁻¹):**1585 (ArC=C), 1659 (C=O), 3020 (ArC–H), 1369 (C–O), 2948 (C–H Str), 3365 (Ar–OH). **¹H NMR** (400 MHz, δ, DMSO, TMS=0): 3.87 (3H, s, 4'-H), 6.85 (2H,d, 3',5'-H, J = 8.56 Hz), 7.37 (2H,d, 2',6'-H, J = 8.56 Hz), 8.17 (1H,s, 2-H), and 6.79 (1H,s, 6-H), 5.02 (Anomeric-H,d, J = 6.2 Hz), 3.33–3.64 (protons of the glucose.), 12.8 (1H, s, –OH) which disappears on D₂O exchange. **¹³C NMR** (400 MHz, δ, DMSO, TMS = 0):C-4, 180.74, C-2157.39, C-5156.47, C-4'153.48, C-6153.06, C-8a 152.47, C-8132.47, C-3',5'115.04, C- 2',6'129.78, C-1'122.45, C-3120.83, C-4a106.85, Sugar carbon; C-1 anomeric carbon of glucose 100.56, C-6(CH₂O) 60.79, C-2, C-3, C-4, C-569.51-77.09. The structure was further authenticated by DEBT analysis enclosed in supplementary copy.

4.3. Glycoside (1a) 7-((2S,3S,4R,5S)-tetrahydro-3,4,5-triacetoxy-6-(acetoxymethyl)-2H-pyran-2-yloxy)- 5,8-diacetoxy-3-(4-methoxyphenyl)-4H-chromen-4-one

The glycoside (**1**) 500 mg was subjected to usual process of acetylation with the addition of acetic anhydride (2–3 mL) and few drops of Conc. H₂SO₄ and kept for 4–5 h at 25 °C to produce (**1a**) 400 mg. The presence of six acetyl groups was confirmed by ¹H

NMR showing the acetyl group protons from 2.14 to 2.65 ppm and there is sharp downfield displacement of the signal for C-5 and C-8 at δ value 6.79–7.07 ppm. The melting point of (**1a**) is 310–312 °C and analyzed for $C_{34}H_{34}O_{17}$ **TOF MS ES⁺**.(m/z): 547.15. Rf value: 0.72, Solvent System; methanol: chloroform (9:1). Elemental Analysis Found (%): C; 57.14, H; 4.37, O; 38.06, and Required: C; 57.01, H; 4.80, O; 37.93, **IR (cm⁻¹)**: 1581 (Ar C=C), 1741 (C=O), 3028 (Ar C-H), 1372 (C-O), 2925 (C-H Str), The IR value 1741 cm⁻¹ (C=O) also clearly indicates the presence of acetyl groups which is the characteristic of phenol acetate and 1190 cm⁻¹ indicates the presence of the ester bond.

4.4. Synthesis of (**1b**)- 5,7,8-trihydroxy-3-(4-methoxyphenyl)-4H-chromen-4-one

Typically, to acid hydrolysis, glycoside (**1**) of 1 g was dissolved in a mixture of methanol (10 mL) and 5% HCl (2–5 drops) and refluxed for 3–4 h. After the usual process of separation, the isolated compounds were subjected to repeated column chromatography thus yielded yellow rosette shape crystals, identified as new isoflavone (**1b**) 500 mg, melting point 225–227 °C and analyzed for $C_6H_{12}O_6$ (TOF MS ES⁺ (m/z): 301.26). Rf value 0.65 (chloroform: methanol 9:1) Elemental Analysis Found (%): C; 64.00, H; 4.03, O; 31.97 and Required: C; 63.21, H; 4.91, O; 30.83. The aqueous portion of the above was subjected to paper chromatography, using *n*-butanol, acetone and water in the ratio 4:1:5, where it was clearly observed that the sugar attached was glucose, with Rf value 0.65. Further the structure was confirmed by UV, IR, ¹H NMR, ¹³C NMR 2-DNMR and mass (TOF MS ES⁺).

IR (cm⁻¹): 1518 (ArC=C), 1659 (C=O), 3080 (ArC-H), 1372 (C-O), 2825(C-H Str), 3368 (Ar-OH). **¹H NMR**: (400 MHz, δ , DMSO, TMS=0): 6.46 (1H,s,6-H), 10.70 (1H,s, 7-OH) Exchangeable with D₂O. **¹³C NMR**: (400 MHz, δ , DMSO, TMS = 0) C-7153.30, C-6131.22, (1b): **TOF MS ES⁺** 2.33e.3 m/z (rel. int): 301[M]⁺ (45.94), 294[M-6H]⁺ (13.12), 285[M-CH₃]⁺ (36.79), 269[M-CH₃-O]⁺ (12.05), 253[M-CH₃-O-O]⁺ (63.63), 237 [M-CH₃-O-O-O]⁺ (10.32), 208 [M-CH₃-O-O-CO₂]⁺ (7.01), 201 [M-C₆H₄CO ring B]⁺ (6.63), Ring B = m/z 100. 187[M-CH₃-O-O-O-C₄H₂]⁺ (61.82), 178[M-C₆H₄CO-C=C]⁺ (28.26), 162[M-C₆H₄CO-C=C-O]⁺ (34.94), 146[M-C₆H₄CO-C=C-O-O]⁺ (22.05), 136[M-C₆H₄CO-C=C-O-C₂H₂]⁺ (7.05), 117[M-CH₃-3O-ring A] (4.91). Ring A = m/z 116. 107[M-C₆H₄CO-C=C-O-C₂H₂-CHO] (59.13), 85[117-2O] (100.

4.5. Synthesis of (**1c**) 5,7,8-triacetoxyoxy-3-(4-methoxyphenyl)-4H-chromen-4-one

The (**1b**) 500 mg was subjected to usual process of acetylation in the presence of acetic anhydride (5–7 mL) and few drops (2–3) of Conc. H₂SO₄, kept for 4–5 h to yield (**1c**) 550 mg. Acetylation yielded colorless triacetate (**1c**), recrystallized from methanol to yield needle shaped crystals, m.p.270–275 °C, analyzed for $C_{22}H_{18}O_9$ (TOF,MS, ES⁺.m/z: 427.20), Rf Value 0.83 (chloroform: methanol 9:1), Elemental Analysis Found (%): C: 61.97, H: 4.26, O: 33.77 and Required: C: 60.51, H: 4.92, O: 31.72. Further the structure was confirmed by U.V. ¹H NMR, ¹³C NMR 2-DNMR and mass (TOF, MS, ES⁺) and ¹H NMR. **IR (cm⁻¹)**: 1514 (ArC=C), 1760 (C=O), 3063 (ArC-H), 1320(C-O), 2870 (C-H Str), 1190, (-COOR). **¹H NMR** (400 MHz, δ , DMSO, TMS=0): 2.31,2.38,2.46 (3H each, s, 8,7 and 5-COCH₃), 7.19 (1H,s, 6-H), 7.87 (1H,s, 2-H), **¹³C NMR** (400 MHz δ , DMSO, TMS = 0): (3 > C=O, 169.42,169.16,167.95), (C-8a 152.07), (C-7, 148.41), (C-5142.96), (C-8, 142.43), (C-6,110.23), (3C-CH₃,21.16,21.07, 20.71).

TOF MS ES⁺ 2.98e.3 m/z (rel. int): 427 [M]⁺ (73.45), 429 [M{2D}]⁺ (5.77), 425[M-2H]⁺ (6.73), 385[M-2H-COCH₃]⁺ (100), 289[M-2H-COCH₃-C₆H₅OCH₃]⁺ (7.45), 269[M{2D}-2H-3 × C₂H₃

O]+(7.88), 273 [M-2H-COCH₃-C₆H₅OCH₃-CH₃]+(12.34), 244[M-2H-COCH₃-C₆H₅OCH₃-CH₃ -CO]+(4.78), 228[M-2H-COCH₃-C₆H₅OCH₃-CH₃ -CO-CH₃]+(3.04), 212[228-O]+(8.01), 181[212-CH₂O](8.01), 126[M-2H-3 × C₂H₃O-ring A]+(5.84), Ring A = m/z142, 117[269-ring B-H]+(5.34). Ring B m/z151.

4.6. Synthesis of (**1d**) and (**1e**)

(**1d**) 7-((2S,3S,4R,5S)-tetrahydro-3,4,5-trimethoxy-6-(methoxymethyl)-2H-pyran-2-yloxy)-5,8-dimethoxyoxy-3-(4-methoxyphenyl)-4H-chromen-4-one.

(**1e**) 7-hydroxy- 5,8-dimethoxy-3-(4-methoxyphenyl)-4H-chromen-4-one.

To a solution of 1000 mg glycoside (**1**), dimethyl sulphate (10 mL), K₂CO₃ (100 mg), in dry acetone and the mixture was refluxed for 5–6 h. The product (**1d**) was processed by usual method, characterized and further subjected to acid hydrolysis (HCl in methanol) to yield (**1e**), purified by column chromatography and recrystallized with methanol to yield fine colorless needle crystals 730 mg (**1e**). Analyzed for $C_{24}H_{26}O_{11}$, (**TOF MS ES⁺**.m/z 491.49) m.p.243–245 °C. Rf value 0.70 (chloroform: methanol 9:1). Elemental Analysis Found (%): C: 59.40, H: 5.78, O: 34.82 and Required: C: 60.90, H: 6.01, O: 33.92. Further the structure was confirmed by U.V. ¹H NMR, ¹³C NMR and mass spectrometry (TOF, MS, ES⁺). **IR (cm⁻¹)**: 1560 (Ar C=C), 1660 (C=O), 3130 (Ar C-H), 1365 (C-O), 2890 (C-H Str). The major functional group has been identified. **¹H NMR**(400 MHz, δ , DMSO, TMS = 0): 3.857 (3H,s, 4'-H), 3.866, 3.938 (3H,s, 5,8-H) 7.193 (1H,s, 6-H), 10.30(1H,s, 7-H) Exchangeable with D₂O. **¹³C NMR** (400 MHz, δ , DMSO, TMS = 0): C-7, 146.31 C-5154.36, C-8142.34, OCH₃, 61.84, C-7 C=O, 169.56.

4.7. Synthesis of (**1f**) 5,8-dimethoxy-3-(4-methoxyphenyl)-4-oxo-4H-chrome-7yl acetate

After the usual process of acetylation of (**1e**) gave white crystalline solid, further recrystallized with methanol to yield (**1f**), m.p.195–198 °C and analyzed for $C_{20}H_{18}O_7$. (**TOF MS ES⁺**.370.35), Rf Value, 0.71, Solvent System, Chloroform: Methanol (9:1), Elemental Analysis Found (%) C; 64.86, H; 4.90 O; 30.24, and Required (%) C; 64.70, H; 5.22, O; 30.92. **IR (cm⁻¹)**: 1560 (Ar C=C), 1760 (C=O), 3130 (Ar C-H), 1365 (C-O), 2890 (C-H Str). The major functional group has been identified. The presence of the acetate group was confirmed by 1760 cm⁻¹ for > C=O group. **¹H NMR** (400 MHz, δ , DMSO, TMS = 0): 2.46 (3H,s, 7-H), **¹³C NMR** (400 MHz, δ , DMSO, TMS = 0): C-7,146.31 C-5154.36, C-8142.34, OCH₃, 61.84, C-7 C=O, 169.56.

4.8. Synthesis of (**1g**) 5,7,8-trihydroxy-3-(4-hydroxyphenyl)-4H-chromen-4-one

Compound (1b) was subjected to demethylation by HBr to yield (**1g**), contains a hydroxyl group at C-4' position The structure was clearly identified and confirmed by ¹H NMR (CDCl₃) at δ values 12.930 ppm singlet exchangeable with D₂O. In the ¹H NMR (CDCl₃) of (**1g**) all the signals remains unchanged except the up field displacement of the signal for the C-3' and C-5' proton from δ value at 7.155–6.970 ppm indicating the presence of one hydroxyl group at C-4' position in ring B.

¹H NMR(400 MHz, δ , DMSO, TMS=0): 6.970 (2H, d, 3',5'-H, J = 8.60 Hz), 7.37 (2H,d, 2',6'-H, J = 8.60 Hz), 8.15 (1H,s, 2-H), 10.70 (1H,s, 7-OH), 12.930 (1H,s, 4'-OH) Exchangeable with D₂O.

4.9. Isolation and identification of glycoside II

The other fractions (85–100) were pooled together to get solid

crystalline mass and were crystallized from absolute alcohol to yield orange needle shaped crystals marked as glycoside (**2**) weighed 1 g. The structure of the compound was characterized and established by UV, IR, ^1H NMR, ^{13}C NMR and mass spectrometry.

4.9.1. Isolation of glycoside-II (**2**) 7-((2S,3S,4R,5S)-tetrahydro-3,4,5-trihydroxy-6-(hydroxymethyl)-2H-pyran-2-yloxy)-6-hydroxy-3-(4-methoxyphenyl)-4H-chromen-4-one

The solid orange needle shaped crystals were obtained and analyzed for $\text{C}_{22}\text{H}_{22}\text{O}_{11}$ ((TOF MS ES⁺, m/z 478.14), m.p.180–183 °C, Rf value 0.54 (chloroform: methanol 9:1) Elemental Analysis Found (%): C: 57.60, H: 4.94, O: 36.86 and Required: C: 57.05, H: 5.28, O: 46.03. Further the structure was confirmed by U.V. ^1H NMR, ^{13}C NMR and mass spectrometry (TOF MS ES⁺).

IR (cm^{-1}): 1566 (ArC=C), 1648 (C=O), 3108 (ArC-H), 1387 (C-O), 2825 (C-H Str), 3300 (Ar-OH). From the IR, data it has been clear that the major functional groups are present e.g. carbonyl, hydroxyl, methyl and aromatic ring. **^1H NMR** (400 MHz, δ , DMSO, TMS = 0): 3.77 (3H, s, 4'-H), 5.03 (Anomeric H, d, J = 6.2 Hz), 6.81 (1H, s, 8-H), 6.85 (2H, d, 3',5'-H, J = 8.56 Hz), 7.37 (2H, d, 2',6', J = 8.56 Hz), 8.08 (1H, s, 5-H), 8.24 (1H, s, 2-H) 3.33–3.64 (Protons of glucose binds anomeric carbon proton). **^{13}C NMR** (400 MHz, δ , DMSO, TMS = 0): C-4, 180.05, C-2157.39, C-4' 156.47, C-2153.48, C-7153.06, C-8a 151.47, C-6142.43, C-2',6'129.78, C-1'125.25, C-3122.83, C-3',5'115.04, C-8, 105.54 C-4a 93.12, Sugar carbon; C-1Anomeric carbon of glucose 100.56, C-6(CH₂O) 60.79, C-2, C-3, C-4, C-569.51-77.09. From the above data the compound was assigned as glycoside (**2**).

4.9.2. Synthesis of (**2a**) 7-hydroxy-3-(4-methoxyphenyl)-4-oxo-4H-chromen-6-yl acetate

The glycoside (**2**) 500 mg was subjected to the usual method of acetylation in the presence of acetic anhydride (3–4 mL) and few drops (2–4) of Conc. H₂SO₄ and refluxed for 4–5 h, followed by acid hydrolysis to yield mono acetate 650 mg, analyzed for $\text{C}_{18}\text{H}_{14}\text{O}_7$ ((TOF MS ES⁺ m/z 478.14), m.p. 163–165 °C and is uncorrected, Rf value 0.70 (chloroform: methanol 9:1) Elemental Analysis Found C: 65.22, H: 4.38, O: 30.41 and Required: C: 65.00, H: 4.98, O: 30.03. **IR** (cm^{-1}): 1560 (Ar (C=C)), 1758 (C=O), 3060 (Ar C-H), 1340(C-O), 1195 (-OCOR). **^1H NMR** (400 MHz, δ , DMSO, TMS = 0): 2.55 (3H, s, 6-Acetyl), 8.13 (1H, s, 5-H), 8.16 (1H, s, 2-H). 12.09 (1H, s, 7-OH) Exchangeable with D₂O. **^{13}C NMR** (400 MHz, δ , DMSO, TMS = 0): C-6140.43, 4'-OCH₃, 55.9, (C=O, C-6, 170.80).

4.9.3. Synthesis of (**2b**) 6,7-diacetoxyoxy-3-(4-methoxyphenyl)-4H-chromen-4-one

Acetylation of (**2a**) yielded fine colorless needles (**2b**) melting point 243–245 °C analyzed for $\text{C}_{20}\text{H}_{16}\text{O}$ (TOF MS ES⁺ m/z 368.09), Rf value 0.55 (chloroform: methanol 9:1). Elemental Analysis Found: C: 65.22, H: 4.04, O:30.41 and Required: C: 64.92, H: 4.38, O: 29.90. **IR**(cm^{-1}): 1570 (Ar (C=C)), 1762 (C=O), 3050 (Ar C-H), 1330(C-O), 1190 (-OCOR). **^1H NMR** (400 MHz, δ , DMSO, TMS = 0): 2.45, 2.54 (3H, s, 6, 7,-OCOCH₃), **^{13}C NMR** (400 MHz, δ , DMSO, TMS = 0): C-7165.64, C-6164.43, (C=O at C-6, C-7, 171.79).

4.9.4. Synthesis of (**2c**) 6,7-dihydroxy-3-(4-methoxyphenyl)-4H-chromen-4-one

Compound (**2**) 350 mg was subjected to usual method of acid hydrolysis in the presence of 5% HCl in methanol and refluxed for 4–5 h to yield yellow solid mass (**2c**) 275 mg, and recrystallized from absolute. The melting point of (**2c**) was 175–180 °C, analyzed for $\text{C}_{16}\text{H}_{12}\text{O}_5$, (TOF MS ES⁺ m/z 285.26), Rf value 0.62 (chloroform: methanol 9:1). Elemental Analysis Found (%): C: 67.60, H: 4.25, O: 28.14 and Required (%) C: 67.60, H: 4.25, O: 28.14 **IR** (cm^{-1}): 1590 (Ar C=C), 1659 (C=O), 3030 (Ar C-H), 1340 (C-O), 3350

(Ar-OH). **^1H NMR** (400 MHz, δ , DMSO, TMS = 0): 6.46(1H, s, 8-H), 8.15(1H, s, 5-H). **^{13}C NMR** (400 MHz, δ , DMSO, TMS = 0): C-5117.48, C-7153.86, C-8a 151.32, C-6142.97, C-8, 110.54.

4.9.5. Synthesis of (**2d**) 7-((2S,3S,4R,5S)-tetrahydro-3,4,5-trimethoxy-6-(methoxymethyl)-2H-pyran-2-yloxy)-6-methoxy-3-(4-methoxyphenyl)-4H-chromen-4-one

Glycoside (**2**) 1 g was subjected to per methylation by usual method (dimethyl sulfate in the presence of K₂CO₃ in dry acetone). After six hours of refluxing, the product was processed. The (**2d**) was isolated, purified by column chromatography and recrystallized with methanol to yield fine colorless needle crystals (700 mg), melting point 234–135 °C analyzed for $\text{C}_{29}\text{H}_{37}\text{O}_{11}$, (TOF MS ES⁺ m/z 561). Rf value 0.66 (chloroform: methanol 9:1). Elemental Analysis Found %: C: 62.02, H: 6.64, O: 31.34, and Required%: C: 61.90, H: 6.92, O: 30.98. **^1H NMR** (400 MHz, δ , DMSO, TMS = 0): 3.83, 3.92 (6H, s, 6, 4'-OCH₃), 5.02 (Anomeric H, d, J = 6.2 Hz.).

4.9.6. Synthesis of (**2e**) 7-hydroxy-6-methoxy-3-(4-methoxyphenyl)-4H-chromen-4-one

The (**2d**) was subjected to acid hydrolysis in the presence of 5% HCl gave fine yellow needles (**2e**) melting point 180–183 °C analyzed for $\text{C}_{17}\text{H}_{14}\text{O}_5$, (TOF MS ES⁺ m/z 298.29), Rf value 0.56 (chloroform: methanol 9:1). Elemental Analysis Found %: C: 68.45, H: 4.73, O: 26.82, and Required %: C: 67.10, H: 5.02, O: 26.98. **^1H NMR** (400 MHz, δ , DMSO, TMS = 0): 3.842, 3.541 (6H, s, 6, 4'-OCH₃), 6.62 (1H, s, 8-H), 9.22 (1H, s, 5-H).

4.9.7. Synthesis of (**2f**) 6-methoxy-3-(4-methoxyphenyl)-4-oxo-4H-chromen-7-yl acetate

The (**2e**) was subjected to the usual process of acetylation (Acetic anhydride in the presence of 10% H₂SO₄) yield colorless needle shape fine crystals (**2f**) melting point 163–165 °C, analyzed for $\text{C}_{19}\text{H}_{14}\text{O}_6$, (TOF MS ES⁺ m/z 321.26), Rf value 0.72 (chloroform: methanol 9:1). Elemental Analysis Found%: C:64.60, H:3.25, O:29.04, and Required:% C: 63.90, H: 4.00, O: 28.93. **^1H NMR** (400 MHz, δ , DMSO, TMS = 0): 2.51 (3H, s, 7, -OCOCH₃), 3.83, 3.92 (6H, s, 6, 4'-OCH₃), **^{13}C NMR** (400 MHz, δ , DMSO, TMS = 0): C-7154.84, (4'-OCH₃, 55.9. 6- OCH₃, 56.34, C=O, C-7173.81).

4.10. Biological activity

4.10.1. Antioxidant activity by DPPH

The solutions of the test compounds were prepared in DMSO, by dissolving 10.24 mg of test compound in 10 mL of DMSO (stock solution). Serial dilutions of the test and standard solutions were made so as to get 200,100, 50, 25, 12.5, 6.25 ppm each. To 1 mL of various concentrations of test solution in DMSO, 1 mL of DPPH solution was added; control was prepared by adding 1 mL of DMSO and 1 mL of DPPH solution and kept 20 min for incubation in dark. After 20 min, the decrease in the absorbance of the test solution (due to quenching of DPPH free radicals) was read at 517 nm and the percentage inhibition was calculated. IC50 values obtained are the concentration of the sample required to scavenge 50% DPPH radical.

4.10.2. Antioxidant activity by ABTS

[2,2'-azinobis-(3-ethylbenzothiazoline-6-sulfonic acid)] Radical Cation Scavenging Method. (Sithisarn and Gritsanapan, 2005).

1 mL of distilled DMSO was added to 0.2 mL of various concentrations of the drug samples or standard, and 0.16 mL of ABTS solution was added to make a final volume of 1.36 mL. Absorbance was measured by spectrophotometer, after 20 min at 734 nm using ELISA reader. Blank was maintained without ABTS. IC50 values obtained are the concentration of the sample required to inhibit

50% ABTS radical mono cation.

4.10.3. Cytotoxic study (MTT assay)

Cytotoxicity was determined in various cell lines, namely MCF-7, MDA-MB-231, HeLa, A-549, PC-3, Vero cell lines using a standard MTT assay method (Mossmann, 1983). 100 μ L of medium containing 5×10^4 cells were seeded per well in a 96-well plates and incubated for 24 h. Solution of compounds was prepared in a medium with 0.2% DMSO. These were exposed to different concentration of test compounds in a range of 200, 100, 50, 25, 12.5, 6.25 μ g/mL, and while blank, positive and negative control cells received the same volume of medium. After 48hrs of incubation media was removed and the cells were incubated with 100 μ L MTT reagent (1 mg/mL) for the next 4 h at 37 $^{\circ}$ C. The coloured formazan was produced by the viable cells and solubilized with 100 μ L DMSO on a vibrator for 5 min. The absorbance was recorded using an ELISA reader at 540 nm and percentage cytotoxicity was calculated. Be sure to read plates within one hour of adding the DMSO. Reagents MTT (3-(4, 5-dimethylthiazol-2-yl)-2, 5-diphenyl tetrazolium bromide (Sigma #M2128): dissolve at 1 mg/mL in PBS, filter and sterilize. PBS = Phosphate buffer saline, pH 7.4.

4.10.4. Cell cycle analysis using propidium iodide

Reagents; Propidium Iodide Staining Solution: 25 μ g/mL PI + 40 μ g/mL RNase A + NP-40 (0.03%) in PBS. 70% ethanol stored in the freezer at -20° C. Wash buffer: PBS +0.1% bovine albumin or serum.

4.10.4.1. Methods. 1×10^6 cells were seeded in petri plates and incubated for 24 h. All the treatments were given and again the cells were incubated for 24 h MCF-7 cells without any treatment served as control and standard drug used was doxorubicin at 2 μ g/mL. Trypsinized the cells and washed with phosphate buffer saline. Added 1 mL of ice cold (-20° C) 70% ethanol into the cell pellet and kept for fixation for 2 h at 4 $^{\circ}$ C. Washed the cells with PBS to remove the alcohol. Added 1 mL of propidium iodide staining solution to cell pellet, mixed well and incubated for 20 min at room temperature in dark. Samples were run in BD Accuri C6 flow cytometer and analyzed using BD Accuri C6 software.

4.11. Molecular docking into DNA binding site of NF-kappaB

Library of 30 possible substituted isoflavones analogues were prepared by using chemdraw ultra 11.0. All ligands were prepared through Auto Dock Tools. The 3D crystal structure of the NF-kappaB was obtained from Protein Data Bank (PDB code: 1NFK) (Borgatti et al., 2011). The 3D structures of NF-kB, p50-p50 homo dimer (from 1NFK), was used for virtual screening (Piccagli et al., 2010). The co-crystallized DNA and water molecules were removed and protein preparation which include minimization was done through UCSF Chimera version 1.8.1 with default parameters (Pettersen et al., 2004). Docking parameters were set to default values on the basis of Lamarckian genetic algorithm principle (Cosconati et al., 2010). Autogrid program of AutoDock suit was used for generation of grid around binding pocket within target protein. DNA fragment was present in the binding pocket of NF kappa B which was removed and grid was generated on same position in the binding cavity. Finally, docking simulation was carried out with AutoDock 4.2. Ligplot and UCSF Chimera version 1.8.1 were used for analysis of docking results (protein ligand interaction) and visualization of docked protein ligand complexes.

Acknowledgments

The authors thank the Faculty of Pharmaceutical Sciences,

Shoolini University Bajhol Solan H.P. (India) for providing research facilities. We also thank to MCOPS Manipal University, Manipal to facilitate part of the research work. We must thank to SAIF, Auvtar Singh and Manish Kumar, Panjab University, Chandigarh, (India) to get spectral data of ^1H NMR, ^{13}C NMR, 2D- NMR (Homo and Hetero Nuclear NMR) and Mass Spectrometry.

Appendix A. Supplementary data

Supplementary data related to this article can be found at <http://dx.doi.org/10.1016/j.phytochem.2017.01.002>.

References

- Ali, A., El-Emary, N., El-Moghazi, M., Darwish, F., Frahm, A., 1983. Three isoflavonoids from *Iris germanica*. *Phytochemistry* 22, 2061–2063.
- Akhter, S., Ahmad, I., Ahmad, M.Z., Ramazani, F., Singh, A., Rahman, Z., Ahmad, F.J., Storm, G., Kok, R.J., 2013. *Curr. Cancer Drug Targets* 13, 362–378.
- Arts, I.C., Hollman, P.C., 2005. Polyphenols and disease risk in epidemiologic studies. *Am. J. Clin. Nutr.* 81, 317S–325S.
- Bhalla, K.N., 2003. Microtubule-targeted anticancer agents and apoptosis. *Oncogene* 22, 9075–9086.
- Bonfills, J., Pinguet, F., Culine, S., Saurvaire, Y., 2004. Cytotoxicity of iridals, triterpenoids from *Iris*. *Plant Med.* 67, 79–81.
- Borgatti, M., Chilin, A., Piccagli, L., Lampronti, I., Bianchi, N., Mancini, I., Marzaro, G., dall'Acqua, F., Guiotto, A., Gambari, R., 2011. Development of a novel furcoumarin derivative inhibiting NF- κ B dependent biological functions: design, synthesis and biological effects. *Eur. J. Med. Chem.* 46, 4870–4877.
- Brasier, A.R., 2006. The NF- κ B regulatory network. *Cardiovasc. Toxicol.* 6, 111–130.
- Bray, F., Ren, J.S., Masuyer, E., Ferlay, J., 2013. Global estimates of cancer prevalence for 27 sites in the adult population in 2008. *Int. J. Cancer* 132, 1133–1145.
- Cassady, J.M., Chan, K.K., Floss, H.G., Leistner, E., 2004. Recent developments in the maytansinoid antitumor agents. *Chem. Pharm. Bull.* 52, 1–26.
- Choudhary, M.I., Nur-e-Alam, M., Baig, I., Akhtar, F., Khan, A.M., Ndögnii, P.Ö., Badarchiin, T., Purevsuren, G., Nahar, N., Atta-ur-Rahman, 2001. Four new flavones and a new isoflavone from *Iris bungei*. *J. Nat. Prod.* 64, 857–860.
- Colic, M., Pavelic, K., 2000. Molecular mechanism of anticancer activity of natural dietetic products. *J. Mol. Med.* 78, 333–336.
- Cosconati, S., Forli, S., Perryman, A.L., Harris, R., Goodsell, D.S., Olson, A.J., 2010. Virtual screening with AutoDock: theory and practice. *Expert Opin. Drug Discov.* 5, 597–607.
- Damme, E., Barre, A., Barbieri, L., Valbonesi, P., Rouge, P., Leuven, F.V., Stirpe, F., Peumans, W., 1997. Type 1 ribosome-inactivating proteins are the most abundant proteins in *Iris hollandica* var. *Professor Blauw* bulbs: characterization and molecular cloning. *Biochem. J.* 324, 963–970.
- Davis, J.N., Kucuk, O., Sarkar, F.H., 1999. Genistein inhibits NF- κ B activation in prostate cancer cells. *Nutr. Cancer* 35, 167–174.
- Freudenthal, R., Romano, A., 2000. Participation of Rel/NF- κ B transcription factors in long-term memory in the crab *Chasmagnathus*. *Brain Res.* 855, 274–281.
- Gilmore, T.D., 2006. Introduction to NF- κ B: players, pathways, perspectives. *Oncogene* 25, 6680–6684.
- Kachroo, K., Razdan, T., Qurishi, M., Khuroo, M., Koul, S., Dhar, K., 1990. Two isoflavones from *Iris kashmiriana* Baker. *Phytochemistry* 29, 1014–1016.
- Kalla, A., Dhar, K., Atal, C., 1977. Search for potential estrogens-synthesis of 4-ethylidene-2-methyl-5, 6, 7, 3', 4', 5'-hexamethoxyisoflavan. *Ind. J. Chem. Sect. B Organ. Chem. Incl. Med. Chem.* 15, 258–259.
- Kalla, A.K., Bhan, M., Dhar, K., 1978. A new isoflavone from *Iris kumaonensis*. *Phytochemistry* 17, 1441–1442.
- Kamata, H., Honda, S.-I., Maeda, S., Chang, L., Hirata, H., Karin, M., 2005. Reactive oxygen species promote TNF α -induced death and sustained JNK activation by inhibiting MAP kinase phosphatases. *Cell* 120, 649–661.
- Kinghorn, A.D., 1994. The discovery of drugs from higher plants. *Biotechnol. Read. Mass* 26, 81.
- Kong, Y., Wang, K., Edler, M.C., Hamel, E., Mooberry, S.L., Paige, M.A., Brown, M.L., 2010. A boronic acid chalcone analog of combretastatin A-4 as a potent anti-proliferation agent. *Bioorg. Med. Chem.* 18, 971–977.
- Lee, S.K., Mbwambo, Z.H., Chung, H., Luveni, L., Gamez, E.J., Mehta, R.G., Kinghorn, A.D., Pezzuto, J.M., 1998. Evaluation of antioxidant potential of natural products. *Comb. Chem. High Throughput Screen.* 1, 35–46.
- Levenson, J.M., Choi, S., Lee, S.-Y., Cao, Y.A., Ahn, H.J., Worley, K.C., Pizzi, M., Liou, H.-C., Sweatt, J.D., 2004. A bioinformatics analysis of memory consolidation reveals involvement of the transcription factor c-rel. *J. Neurosci.* 24, 3933–3943.
- Mossmann, T., 1983. Rapid colorimetric assay for cellular growth and survival: application to proliferation and cytotoxicity assays. *J. Immunol. Methods* 65, 55–63.
- Mattson, M.P., Camandola, S., 2001. NF- κ B in neuronal plasticity and neurodegenerative disorders. *J. Clin. Investig.* 107, 247.
- Meffert, M.K., Chang, J.M., Wiltgen, B.J., Fanselow, M.S., Baltimore, D., 2003. NF- κ B functions in synaptic signaling and behavior. *Nat. Neurosci.* 6, 1072–1078.
- Merlo, E., Freudenthal, R., Romano, A., 2002. The I κ B kinase inhibitor sulfasalazine

- impairs long-term memory in the crab *Chasmagnathus*. *Neuroscience* 112, 161–172.
- Nadaroglu, H., Demir, Y., Demir, N., 2007. Antioxidant and radical scavenging properties of *Iris germanica*. *Pharm. Chem. J.* 41, 409–415.
- Nasim, S., Baig, I., Jalil, S., Orhan, I., Sener, B., Choudhary, M.I., 2003. Anti-inflammatory isoflavonoids from the rhizomes of *Iris germanica*. *J. Ethnopharmacol.* 86, 177–180.
- Parr, A.J., Bolwell, G.P., 2000. Phenols in the plant and in man. The potential for possible nutritional enhancement of the diet by modifying the phenols content or profile. *J. Sci. Food Agric.* 80, 985–1012.
- Patel, J.M., 2008. A Review of Potential Health Benefits of Flavonoids.
- Perkins, N.D., 2007. Integrating cell-signalling pathways with NF- κ B and IKK function. *Nat. Rev. Mol. Cell Biol.* 8, 49–62.
- Pettersen, E.F., Thomas, D., Goddard, Conrad, C., Huang, Gregory, S., Couch, Daniel, M., Greenblatt, Elaine, C., Meng, Thomas, E., Ferrin, 2004. UCSF Chimera—a visualization system for exploratory research and analysis. *J. Comput. Chem.* 13, 1605–1612.
- Piccagli, L., Borgatti, M., Nicolis, E., Bianchi, N., Mancini, I., Lampronti, I., Vivaldi, D., Dall'Acqua, F., Cabrini, G., Gambari, R., 2010. Virtual screening against nuclear factor κ B (NF- κ B) of a focus library: identification of bioactive furocoumarin derivatives inhibiting NF- κ B dependent biological functions involved in cystic fibrosis. *Bioorg. Med. Chem.* 18, 8341–8349.
- Piccagli, L., Fabbri, E., Borgatti, M., Bianchi, N., Bezzetti, V., Mancini, I., Nicolis, E., Dehecchi, C.M., Lampronti, I., Cabrini, G., 2009. Virtual screening against p50 NF- κ B transcription factor for the identification of inhibitors of the NF- κ B–DNA interaction and expression of NF- κ B upregulated genes. *ChemMedChem* 4, 2024–2033.
- Sithisarn, P., Gritsanapan, W., 2005. Free radical scavenging activity and total flavonoids content of siamese neem tree leaf aqueous extract from different locations. *J. Pharm. Sci.* 32, 31–35.
- Suthar, S.K., Jaiswal, V., Lohan, S., Bansal, S., Chaudhary, A., Tiwari, A., Alex, A.T., Joesph, A., 2013. Novel quinolone substituted thiazolidin-4-ones as anti-inflammatory, anticancer agents: design, synthesis and biological screening. *Eur. J. Med. Chem.* 63, 589–602.
- Tian, B., Brasier, A.R., 2003. Identification of a nuclear factor kappa B-dependent gene network. *Recent Prog. Hormone Res.* 58, 95–130.
- Tsao, A.S., Kim, E.S., Hong, W.K., 2004. Chemoprevention of cancer. *CA Cancer J. Clin.* 54, 150–180.
- Valachovicova, T., Slivova, V., Bergman, H., Shuherk, J., Sliva, D., 2004. Soy isoflavones suppress invasiveness of breast cancer cells by the inhibition of NF- κ B/AP-1-dependent and-independent pathways. *Int. J. Oncol.* 25, 1389–1395.
- Walle, T., 2007. Methylation of dietary flavones greatly improves their hepatic metabolic stability and intestinal absorption. *Mol. Pharm.* 4, 826–832.
- Wallström, P., Wirfält, E., Janzon, L., Mattisson, I., Elmståhl, S., Johansson, U., Berglund, G., 2000. Fruit and vegetable consumption in relation to risk factors for cancer: a report from the Malmö Diet and cancer study. *Public Health Nutr.* 3, 263–271.
- Williams, C.A., Harborne, J.B., Colasante, M., 1997. Flavonoid and xanthone patterns in bearded *Iris* species and the pathway of chemical evolution in the genus. *Biochem. Syst. Ecol.* 25, 309–325.
- Xiao, Z.-P., Peng, Z.-Y., Peng, M.-J., Yan, W.-B., Ouyang, Y.-Z., Zhu, H.-L., 2011. Flavonoids health benefits and their molecular mechanism. *Mini Rev. Med. Chem.* 11, 169–177.
- Yarishkin, O.V., Ryu, H.W., Park, J.-Y., Yang, M.S., Hong, S.-G., Park, K.H., 2008. Sulfonate chalcone as new class voltage-dependent K⁺ channel blocker. *Bioorg. Med. Chem. Lett.* 18, 137–140.